
Journal of Engineering Mathematics **50:** 399–414, 2004.

Delayed thermal explosion in flammable gas containing fuel droplets: asymptotic analysis

I. GOLDFARB, S. SAZHIN[1] and A. ZINOVIEV[2]
Department of Mathematics, Ben-Gurion University of the Negev, P.O.B. 653, Beer-Sheva 84105, Israel, E-mail: goldfarb@cs.bgu.ac.il; [1]*School of Engineering, Faculty of Science and Engineering, The University of Brighton, Brighton BN2 4GJ, UK, E-mail: S.Sazhin@bton.ac.uk;* [2]*Department of Software Engineering, Negev Academic College of Engineering, 71 Bazel Street, Beer-Sheva 84100, Israel, E-mail: annaz@nace.ac.il*

Received 30 June 2003; accepted in revised form 24 February 2004

Abstract. The problem of thermal explosion in a flammable gas mixture with addition of volatile fuel droplets is studied based on the asymptotic method of integral manifolds. The model for the radiative heating of droplets takes into account the semitransparency of droplets. A simplified model for droplet heat-up is used. The results of the analysis are applied to the modelling of thermal explosion in diesel engines. Two distinct dynamical situations have been considered, depending on the initial droplet concentration. These are 'far zone' (small initial liquid volume fraction and small droplet radii) and 'near zone' (large initial liquid volume fraction and large droplet radii). The conditions of the first zone are typical for the areas in the combustion chamber which are far from the fuel injectors, while the conditions of the second zone are typical for the areas in the combustion chamber which are relatively close to the fuel injectors. It has been pointed out that small droplets' heating and evaporation time in the far zone is smaller than the chemical ignition delay of the fuel vapor/air mixture. The total ignition delay decreases with increasing initial gas temperature. In the near zone for large droplets, the process starts with the initial gas cooling and slight heating of droplets. This is followed by a relatively slow heating of gas due to the chemical reaction, and further droplet heating. The total ignition delay in the near zone is larger than in the far zone. It is expected that before thermal explosion in the near zone takes place, the droplets break up and are removed from this zone. In optically thick gas effects of thermal radiation are negligible for small droplets but are noticeable for large droplets.

Key words: asymptotics, diesel engine, method of integral manifolds, spray combustion

1. Introduction

The problem of thermal explosion of flammable gas containing fuel droplets, and its numerous applications, have been widely discussed in the literature [1, Chapter 6], [2]. Semenov [3] was perhaps the first to develop the basic theory of the phenomenon of thermal explosion. Since that time more and more complicated models have been suggested 4 [5, Chapters 10–12], [6], [7, Chapter 7], [8], [9]. The analysis of these models has been mainly performed using modern computers. They have been incorporated into various CFD packages and allowed to take into account heat and mass transfer and combustion processes in the mixture of gas and fuel droplets in a self-consistent way [10–13]. This approach, however, is not particularly helpful in aiding understanding of the relative contribution of various processes. An alternative approach to the problem is to analyze the equations in some limiting cases. This cannot replace CFD methods but can complement them. For example, the geometrical asymptotic method of integral manifolds can be used [14]. This method was successfully applied to modeling self-ignition problems [15–18].

Sazhin *et al.* [19] applied this method to the specific problem of modeling the ignition process in diesel engines [20]. These authors attempted to combine the analytical approach, based on the integral-manifold method, and CFD simulations of the process, based on the CFD package VECTIS. The analytical analysis in this paper took into account both convective and radiative heating of droplets, but it was assumed that the droplet temperature was constant (heat-up period had been completed). The radiative-heating model used in this paper was based on the assumption that fuel droplets are grey opaque spheres. Also, the chemical reaction term, used in the analytical model, was assumed in the one-step Arrhenuis form. The latter might be a serious oversimplification as the combustion process in diesel engines involves hundreds of species and chemical reactions [21–24]. The analysis of these reactions is beyond the capacity of most CFD codes and a number of reduced mechanisms have been suggested [25–27]. One mechanism widely used in CFD codes is the so-called Shell model [28]. Sazhin *et al.* [19] attempted to approximate the contribution of the reduced chemistry, described by the Shell model, in the enthalpy equation in the Arrhenuis form with the time-dependent pre-exponential factor $A(t)$. However, this had limited success as the function $A(t)$ implicitly depended on fuel vapor and oxygen concentrations. The main argument supporting the application of the Arrhenuis form of the chemical term is that the physical ignition delay for average sized droplets in diesel engines (due to heating and evaporation of droplets) is generally longer than the chemical ignition delay (due to chemical reactions, [13]).

The present paper is focused on further development of the model used in [19]. Firstly, the assumption that droplets are opaque gray spheres is replaced by a more realistic assumption that droplets are semi-transparent spheres. Secondly, the process of droplet heat-up is taken into account. Thirdly, the equations are investigated for a wide range of parameters typical for diesel engines (not just average values as done in [19]).

The problem of droplet heating taking into account their semi-transparency has been considered in [29] [30, Chapter 2]. The models developed by these authors, however, were too complicated not only for analytical studies, but also for implementation into CFD codes. Dombrovsky *et al.* [31] seem to be the first to describe the process in a form simple enough for implementation into CFD codes and analytical studies. Their model is based on the geometrical optics approximation, which is valid for typical diesel-fuel droplets with radii more than about 3 μm. The final expression for the absorption coefficient of droplets was presented in the form $\left(a\, R_d^b\right)$, where R_d is droplet radius, a and b are quadratic functions of gas temperature. This model is used in our paper.

The problem of droplet heat-up is well known and has been widely discussed in the literature [32, 7]. In our case, however, we are not interested in the details of the process, but just need to take into account the fact that, at the initial stage (droplet temperature is equal to room temperature), all heat is spent on droplet heating. When the droplet temperature becomes equal to the boiling temperature all heat is spent on droplet evaporation. A simplified model originally suggested in [33] takes into account both of these effects. This will be used in our paper.

The analytical analysis reported in [19] was based on average values of parameters in diesel engines. These values, however, can vary by several orders of magnitude within the combustion chamber [20]. This will be taken into account in the present paper. The focus will be on the initial stage of the thermal explosion. Two main dynamical scenarios, depending on the initial concentration of the fuel droplets, will be identified. These correspond to two zones in the combustion chamber: a far zone (far from the droplet injector), where the initial droplet concentration is low, and a near zone (close to the droplets injector), where the initial droplet

concentration is high. Note that the immediate vicinity of the nozzle, where liquid jet has not yet disintegrated into droplets, is beyond the scope of our analysis.

The main equations and approximations, used in the analysis, are presented and discussed in Section 2. In Section 3 these equations are presented in dimensionless forms convenient for analytical analysis. Analysis of the equations, using the asymptotic method of invariant manifolds, is presented in Section 4. The results of this section are then applied to the analysis of the ignition process in conditions relevant to diesel engines (Section 5). The main results of the paper are summarized in Section 6.

2. Problem statement

The following main physical assumptions have been used. The combustible gas mixture contains evaporating ideal spherical droplets of fuel. These liquid droplets form a mono-disperse spray, and the medium is assumed to be spatially homogeneous. We ignore the variations in pressure in the enclosure, and their influence on the combustion process. Heat flux from the burning gas to droplets is assumed to consist of two components: convection and radiation. The energy needed for heating fuel vapor from the droplet temperature to gas temperature is ignored. We assume that the thermal conductivity of the liquid phase is much greater than that of the gas phase and the volume fraction of the liquid phase is much less than that of the gas phase. The heat-transfer coefficient in the liquid-gas mixture is assumed to be controlled by the thermal properties of the gas phase. External heat losses are ignored (adiabatic approach). Fuel drops are semi-transparent and the diffraction parameter is large (geometrical-optics approximation is valid). Combustion takes place in the gas phase only. Combustion is modeled as a one-step first-order exothermic reaction with gaseous fuel as a deficient reactant. Droplets are assumed to be stationary or almost stationary (Re $\ll 1$) [34].

Under these assumptions we can write the energy balance equation for the gas phase in the following general form

$$C_{pg}\rho_g\varphi_g\frac{\mathrm{d}T_g}{\mathrm{d}t} = c_f Q_f \mu_f \varphi_g A \exp\left(-\frac{E}{R_u T_g}\right) - 4\pi R_d^2 n_d \left(q_c + q_r\right), \tag{1}$$

where T is the temperature (K), c_f the molar concentration of the combustible component in gaseous mixture (kmol/m^3); R_d the radius of the droplets (m), A a constant pre-exponential factor (1/s), E the activation energy (J/kmol), R_u the universal gas constant, C the specific heat capacity (J/kg/K), φ the volumetric phase content (dimensionless); ρ the density (kg/m^3), q the heat flux (W/m^2); μ the molar mass (kg/kmol); Q_f the specific (per unit mass) combustion energy (J/kg); n_d the number of droplets per unit volume (1/m^3); t the time. Subscripts: g refers to gas mixture; f refers to combustible gas component of the mixture (fuel); d refers to liquid droplets; p refers to constant pressure; r refers to radiation; c refers to convection.

The variations of gas density with time are ignored. This is justified by the fact that spray injection in diesel engines takes place near the top dead center when density variations are minimal.

The heat depleted as a result of gaseous fuel burning is spent on the fuel droplets heating and their further evaporation. The droplet average temperature equation reads as:

$$C_d m_d \frac{\mathrm{d}T_d}{\mathrm{d}t} = 4\pi R_d^2 \left(q_c + q_r\right) \zeta(T_d), \tag{2}$$

where m_d is the droplet mass, the right-hand side of Equation (2) becomes zero when the liquid-fuel temperature reaches the boiling point T_b. The parameter $\zeta(T_d)$ takes into account the fraction of heat spent on droplet heating. Following [33] it is taken in the form:

$$\zeta(T_d) = \frac{T_b - T_d}{T_b - T_{d0}}, \tag{3}$$

where T_b, T_d and T_{d0} are the boiling, current and initial temperatures of droplets, respectively; $\zeta(T_d)$ decreases from 1 to 0 when T_d increases from T_{d0} to T_b. This reflects the decrease of heat spent on droplet heating when the droplet temperature increases. The range of T_d under consideration is the interval $[T_{d0},\ T_b]$.

The rate of fuel evaporation is described as:

$$\frac{\mathrm{d}m_d}{\mathrm{d}t} = -\frac{4\pi R_d^2}{L}\left(q_c + q_r\right)\left(1 - \zeta(T_d)\right), \tag{4}$$

where L is the latent heat of evaporation (J/kg); we took into account that the fraction of heat spent on droplet evaporation is proportional to $(1 - \zeta(T_d))$.

The combustible gas-component content is controlled by oxidation (flammable substance consumption) and droplet evaporation (fuel vapor source). We assume that the gas represents a well-stirred combustible mixture. The combustible gas concentration equation is given by:

$$\varphi_g \frac{\mathrm{d}c_f}{\mathrm{d}t} = -c_f \varphi_g A \exp\left(-\frac{E}{R_u T_g}\right) + \frac{4\pi R_d^2 n_d}{L\mu_f}\left(q_c + q_r\right)\left(1 - \zeta(T_d)\right). \tag{5}$$

Remembering our assumption that Re $\ll$ 1, we have Nu $=$ 2 [35, Chapter 22], [36]. This allows us to simplify the expression for q_c to the term, proportional to the difference between gas and droplet temperatures. The coefficient can be derived on the basis of the external heat-transfer problem for the droplet (see for example [1]). The expression reads:

$$q_c = \frac{\lambda_g}{R_d}(T_g - T_d), \quad \lambda_g = \sqrt{\frac{T_g}{T_{g0}}}, \tag{6}$$

where λ_{g0} is the gas thermal conductivity at $T_g = T_{g0}$.

In deriving Equation (6), we took into account the temperature dependence of the gas thermal conductivity [35, Chapter 9]. The approximation Nu $=$ 2 is expected to be valid in most of the diesel-engine combustion chamber, where the relative velocity of droplets and entrained air is expected to be small [34]. This approximation can be poor near the nozzle (fuel injector), where the dependence of Nu on Re needs to be taken into account.

The expression for q_r can be written as $q_r = \sigma\, Q_{ai}\left(T_{\text{ext}}^4 - T_d^4\right)$, where σ is the Stefan-Boltzmann constant, Q_{ai} is the average efficiency factor of absorption, T_{ext} is the external temperature (alternative presentations of q_r were discussed in [37, 38]. In the case of an optically thick gas we can assume that $T_{\text{ext}} = T_g$. Otherwise, T_{ext} can be considered as constant, and the whole analysis would be simplified. The values of Q_{ai} depend on the physical model chosen. Following [31] we use the following approximate expression $Q_{ai} = a\, R_d^b$, where a and b are quadratic functions of the external (gas) temperature. This expression was derived by curve fitting for 5 μm $\leq R_d \leq$ 50 μm 5 and 1000 K $\leq T_g \leq$ 3000 K (realistic values for diesel engines). The analysis will be focused mainly on the case of an optically thick gas when $T_{\text{ext}} = T_g$. Parameter b is a rather weak function of T_g and we can assume that $b = 0{\cdot}6$. The expression for a as the first approximation can be presented as a linear function in the form

$a = 10^3 k_{01} - k_{11} T_g$. The values of k_{01} and k_{11} depend on units of R_d. If (μm) are used then $k_{01} = 7 \times 10^{-5}$, $k_{11} = 2 \times 10^{-5}$ K^{-1}; if (m) are used then $k_{01} = 0{\cdot}28$, $k_{11} = 0{\cdot}08$ K^{-1}. As a result the expression for q_r reads:

$$q_r = \sigma R_d^b \left(10^3 k_{01} - k_{11} T_g\right) \left(T_g^4 - T_d^4\right). \tag{7}$$

More accurate approximations for a and b in a wider range of droplet radii and gas temperatures, and for various diesel fuels were reported in [39]. Equation (7) is consistent with these new results. Results of application of the expression $Q_{ai} = a\, R_d^b$ in a CFD code were reported in [40].

The system of governing equations is closed with the initial conditions of the form:

$$t = 0 : T_g = T_{g0}; \quad T_d = T_{d0}; \quad c_f = c_{f0}; \quad R_d = R_{d0}. \tag{8}$$

The contribution of surface tension is ignored. Even for extremely small diesel fuel droplets with radii about 10^{-6} m, the surface-tension effects are expected to increase the pressure inside the droplets by less than 1%.

3. Non-dimensionalization

Equations (1)–(7) can be rewritten in the dimensionless form:

$$\gamma \frac{\mathrm{d}\theta_g}{\mathrm{d}\tau} = H_{HR}(\eta, \theta_g) - \varepsilon_1 r \; H_{HL}(r, \theta_g, \theta_d), \tag{9}$$

$$\frac{\mathrm{d}\eta}{\mathrm{d}\tau} = -H_{HR}(\eta, \theta_g) + \psi_f \, \varepsilon_1 r \; (1 - \zeta\,(\theta_d))\, H_{HL}(r, \theta_g, \theta_d), \tag{10}$$

$$\frac{\mathrm{d}\theta_d}{\mathrm{d}\tau} = \frac{\varepsilon_3}{r^2} H_{HL}(r, \theta_g, \theta_d) \zeta\,(\theta_d)\,, \tag{11}$$

$$\frac{\mathrm{d}r^3}{\mathrm{d}\tau} = -\varepsilon_1 \varepsilon_2 \, r \, H_{HL}(r, \theta_g, \theta_d)\,(1 - \zeta\,(\theta_d))\;. \tag{12}$$

The term H_{HR} is responsible for heat release due to exothermic chemical reaction:

$$H_{HR}(\eta, \theta_g) = \eta \exp\left(\frac{\theta_g}{1 + \beta\theta_g}\right). \tag{13}$$

The term H_{HL} reflects the impact of internal heat losses in the system under consideration (via convection and radiation):

$$H_{HL}(r, \theta_g, \theta_d) \;=\; \left[\left(\theta_g - \theta_d\right)\sqrt{1 + \beta\theta_g} + \frac{\varepsilon_4}{4\beta} r^{b+1} \left(\nu - \left(1 + \beta\theta_g\right)\right) \left(\left(1 + \beta\theta_g\right)^4 - (1 + \beta\theta_d)^4\right)\right]. \tag{14}$$

The parameter $\zeta\,(\theta_d)$ is the modified form of the parameter (3), and it is given by:

$$\zeta\,(\theta_d) = \left(\frac{\theta_b - \theta_d}{\theta_b - \theta_{d0}}\right). \tag{15}$$

The following dimensionless parameters have been introduced:

$$\beta = \frac{R_u T_{g0}}{E}, \gamma = \frac{C_{pg} T_{g0} \rho_{g0}}{c'_{f0} Q_f \mu_f}\beta, c'_f = \frac{\varphi_d \rho_{d0}}{\mu_f}, \varepsilon_1 = \frac{4\pi R_{d0} \lambda_{g0} n_d T_{g0} \beta \exp(1/\beta)}{A c'_f Q_f \mu_f \varphi_g},$$
$$\varepsilon_2 = \frac{c'_f Q_f \mu_f \varphi_g}{(4/3)\pi R_{d0}^3 n_d \rho_{d0} L}, \varepsilon_3 = \frac{3\lambda_{g0} \exp(1/\beta)}{A C_d \rho_{d0} R_{d0}^2}, \varepsilon_4 = \frac{4\sigma k_{11} T_{g0}^4 R_{d0}^{b+1}}{\lambda_{g0}}, \psi_f = \frac{Q_f}{L}, \quad (16)$$
$$\nu = \frac{k_{01} 10^3}{k_{11} T_{g0}}, \phi_g = \frac{T_g - T_{g0}}{\beta T_{g0}}, \phi_d = \frac{T_d - T_{g0}}{\beta T_{g0}}, \eta = \frac{c_f}{c'_f}, r = \frac{R_d}{R_{d0}}, \tau = \frac{t}{t_{\text{react}}},$$
$$t_{\text{react}} = A^{-1} \exp(1/\beta).$$

Here t_{react} is the time required for the reactant concentration to fall by a factor (e) from its initial value under the isothermal conditions; c'_f is the fuel vapor concentration after all droplets have evaporated but not burnt.

Parameters β and γ are the conventional parameters of the Semenov theory of thermal explosion [3]: β is the reduced initial temperature, γ represents the final dimensionless adiabatic temperature of the thermally insulated system after the explosion has been completed. Characteristic values of the parameters β and γ are small compared with unity for most gaseous mixtures due to the high exothermicity of the chemical reaction and high activation energy. Parameter ε_1 describes the competition between the combustion and evaporation processes. Parameter ε_2 relates the heat released during combustion and energy needed to evaporate all fuel droplets. Parameter ε_3 is the ratio of t_{react} and the characteristic droplet heating time. Parameter ε_4 is proportional to the ratio of radiative and convective fluxes. Parameter ψ_f shows the characteristics of the fuel (ratio of specific combustion energy and latent heat of vaporization). For diesel fuels $\psi_f \gg 1$.

For applications in diesel engines we also can assume that the initial concentration of gaseous fuel inside the combustion chamber is small, so that $\eta_0 = 0$. Under this assumption the initial conditions (8) are given in dimensionless form by:

$$\tau = 0 : \theta_g = 0; \quad \theta_d = \theta_{d0}; \quad \eta = 0; \quad r = 1. \quad (17)$$

4. Analysis

The system of Equations (9)–(12) together with the initial conditions (17) can be solved numerically. Although these solutions can be useful for engineering applications, they have a number of limitations, as discussed in the Introduction. In the present paper an alternative approach to the analysis of the system of Equations (9)–(12), (17) will be used. This will be based on the asymptotic method of invariant manifolds developed in [14]. In this method a system of ODEs is treated as a multi-scale system with a small parameter, and includes slow and fast subsystems. The dynamic behavior is described by the typical system trajectories, which in turn can be predicted using the slow invariant manifold. A trajectory can be decomposed into 'fast' parts (away from the slow manifold) and 'slow' parts (in the neighborhood of the slow manifold). The slow invariant manifold can be found in powers of the small parameter. The analysis of the present paper is restricted to the zeroth-order approximation of the slow invariant manifolds. The zeroth-order approximation of the slow invariant manifold is called the slow surface.

For the system of Equations (9)–(12) two integrals can be found. To obtain one of the integrals, Equations (11) and (12) are combined to give:

$$\frac{\mathrm{d}\theta_d}{\mathrm{d}r^3} = -\frac{\varepsilon_3}{\varepsilon_1\varepsilon_2}\frac{1}{r^3}\frac{\zeta\left(\theta_d\right)}{1-\zeta\left(\theta_d\right)}.$$

Integration of this equation subject to the initial condition (17) gives a relation between the temperature and radius of the droplets:

$$r^3\left(\theta_d\right) = \left[\mathrm{e}^{(\theta_d-\theta_{d0})}\left(\frac{\theta_b-\theta_d}{\theta_b-\theta_{d0}}\right)^{(\theta_b-\theta_{d0})}\right]^{\frac{\varepsilon_1\varepsilon_2}{\varepsilon_3}}. \tag{18}$$

To find the second integral of the system, Equations (9) and (10) are combined as:

$$\frac{\mathrm{d}\left(\gamma\theta_g+\eta\right)}{\mathrm{d}\tau} = \varepsilon_1 r\ \left(\psi_f\left(1-\zeta\left(\theta_d\right)\right)-1\right)\ H_{HL}(r,\theta_g,\theta_d).$$

This equation can be now combined with Equations (11) or (12) to give:

$$\frac{\mathrm{d}\left(\gamma\theta_g+\eta\right)}{\mathrm{d}\theta_d} = \frac{\varepsilon_1}{\varepsilon_3}r^3\left(\theta_d\right)\frac{\left(\psi_f\left(1-\zeta\left(\theta_d\right)\right)-1\right)}{\zeta\left(\theta_d\right)},$$

with $r^3\left(\theta_d\right)$ given by Equation (18). Integration of the last equation subject to the initial conditions (17) gives:

$$\eta\left(\theta_g,\theta_d\right) = -\gamma\theta_g + \frac{\varepsilon_1}{\varepsilon_3}\int_{\theta_{d0}}^{\theta_d} r^3\left(s\right)\frac{\left(\psi_f\left(1-\zeta\left(s\right)\right)-1\right)}{\zeta\left(s\right)}\,\mathrm{d}s. \tag{19}$$

Equations (18) and (19) can replace Equations (12) and (10), respectively. This reduces the original system (9)–(12) to the two-dimensional system (9) and (11) in the$\left(\theta_g,\theta_d\right)$-plane, together with the additional functional relations (18) and (19).

We will concentrate on analyzing the delay regimes, *i.e.*, regimes characterized by a delay period before the occurrence of the final blow-up. These are particularly important for the applications. An important feature of such regimes is that their time histories are determined by the very initial stages of the thermal explosion when the temperatures are comparatively low ($\theta_g \propto O(1)$). Remembering that $\beta \ll 1$, this allows us to apply the Frank-Kamenetskii approximation [41]:

$$\exp\left(\frac{\theta_g}{1+\beta\theta_g}\right) \approx \exp\left(\theta_g\right).$$

The additional simplification used in this paper is a zeroth-order approximation of the heat-loss function H_{HL} with respect to the small parameter β (this also works well at comparatively low temperatures where $\beta\theta_g < 1$). Under these assumptions, Equations (13)–(14) can be re-written as:

$$H_{HR}(\eta,\theta_g) \approx H_{HR}^{FK} \stackrel{\text{def}}{=} \eta\exp\left(\theta_g\right), \tag{20}$$

$$H_{HL}(\eta,\theta_g,\theta_d) \approx H_{HL}^{\text{app}} \stackrel{\text{def}}{=} \left(\theta_g-\theta_d\right)\left[1+\varepsilon_4\left(\nu-1\right)r^{b+1}\right]. \tag{21}$$

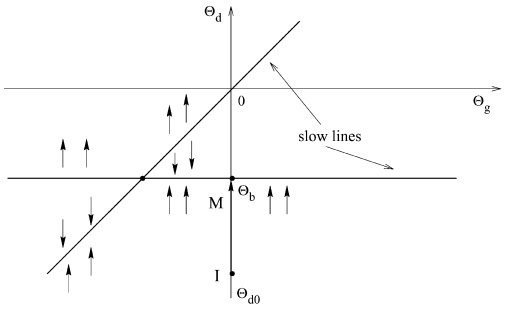

Figure 1. The slow lines and the phase trajectory IM in (θ_d, θ_g) space for the system of Equations (22)–(24) (far zone). Arrows show stability of the slow lines.

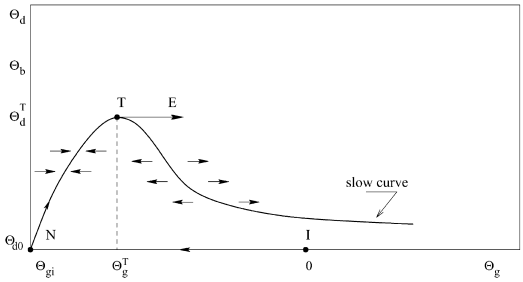

Figure 2. The slow curve and the phase trajectory INTE in (θ_d, θ_g) space for the system of Equations (22)–(24) (near zone). Arrows show stability of the slow curve. The value θ_d^T lies in the interval (θ_{d0}, θ_b).

The reduced system is given by:

$$\gamma \frac{\mathrm{d}\theta_g}{\mathrm{d}\tau} = H_{HR}^{FK}\left(\eta\left(\theta_g, \theta_d\right), \theta_g\right) - \varepsilon_1 r\left(\theta_d\right) \; H_{HL}^{\mathrm{app}}\left(r\left(\theta_d\right), \theta_g, \theta_d\right) \stackrel{\mathrm{def}}{=} F\left(\theta_g, \theta_d\right), \tag{22}$$

$$\frac{\mathrm{d}\theta_d}{\mathrm{d}\tau} = \frac{\varepsilon_3}{r^2\left(\theta_d\right)} H_{HL}^{\mathrm{app}}\left(r\left(\theta_d\right), \theta_g, \theta_d\right) \zeta\left(\theta_d\right) \stackrel{\mathrm{def}}{=} G\left(\theta_g, \theta_d\right), \tag{23}$$

subject to

$$\tau = 0 : \theta_g = 0; \;\; \theta_d = \theta_{d0}, \tag{24}$$

where H_{HR}^{FK}, H_{HL}^{app}, $\eta\left(\theta_g, \theta_d\right)$ and $r\left(\theta_d\right)$ are given by Equations (20), (21), (19) and (18), respectively.

The integral manifolds method can be applied to the analysis of the initial-value problem (22)–(24) in the phase-plane (θ_g, θ_d) if one of the variables is fast while the other is slow. The initial hierarchy of the system is determined by the ratio $\varepsilon_3\gamma/\varepsilon_1$. This is the ratio between volumetric heat capacities of the gaseous and liquid phases: $\varepsilon_3\gamma/\varepsilon_1 = \left(C_{pg}\rho_{g0}\varphi_{g0}\right) / \left(C_d\rho_d\varphi_{d0}\right)$. The analysis will be performed for $\varepsilon_3\gamma/\varepsilon_1 \gg 1$ and $\varepsilon_3\gamma/\varepsilon_1 \ll 1$.

4.1. THE CASE $\varepsilon_3\gamma/\varepsilon_1 \gg 1$

In this situation initially θ_d is a rapidly varying variable, and θ_g is a slowly varying variable. The slow curve of the system of Equations (22)–(24) is defined by the quasi-steady-states of the fast Equation (23) $G\left(\theta_g, \theta_d\right) = 0$. Remembering Equations (18) and (21), we observe that the slow curve $G\left(\theta_g, \theta_d\right) = 0$ consists of the two straight lines:

$$\theta_g - \theta_d = 0\,, \;\; \theta_b - \theta_d = 0 \tag{25}$$

The slow curve may attract or repel the phase trajectories. This is determined by the stability of the slow curve controlled by the sign of $\left(\partial G \big/ \partial\theta_d\right)$. The conditions $\left(\partial G \big/ \partial\theta_d < 0\right)$ and $\left(\partial G \big/ \partial\theta_d > 0\right)$ define the stable (attracting) and unstable (repelling) manifolds, respectively. The condition for marginal stability $G = \partial G \big/ \partial\theta_d = 0$ is given by the intersection of the two invariant lines (25). Stability of the invariant lines (25) and the phase trajectory is illustrated in Figure 1. One can see that in the case under consideration when cool droplets

are injected into a hot gas $\left(\theta_{d0} < \theta_b < \theta_{g0} = 0\right)$, the phase trajectory IM starting at the initial point $\mathrm{I}\left(\theta_g = 0, \theta_d = \theta_{d0}\right)$ moves upwards until it reaches the stable part of the invariant line $\theta_d = \theta_b$ (at the end point M). That means that the droplet temperature increases rapidly from the initial value θ_{d0} up the boiling value θ_b. The latter is its final steady state. As follows from Equation (18), the droplet radius decreases as the droplet temperature θ_d increases, and it becomes equal to zero at the boiling point: $r\left(\theta_b\right) = 0$. Once the evaporation has been completed, the system of Equations (22)–(24) degenerates to the conventional gaseous explosive system with no presence of liquid phase (the evaporation of the fuel droplets is completed and the source of the internal heat losses of the system disappears):

$$\gamma \frac{\mathrm{d}\theta_g}{\mathrm{d}\tau} = \eta\left(\theta_g, \theta_b\right) \exp\left(\theta_g\right), \quad \theta_g\left(\tau = 0\right) = 0, \tag{26}$$

where $\eta\left(\theta_g, \theta_b\right)$ is given by Equation (19) with $\theta_d = \theta_b$. Equation (26) represents the classical Semenov model without heat losses with reactant consumption $\eta\left(\theta_g, \theta_b\right)$ taken into account via Equation (19).

This means that the dynamic behavior of the system (22)–(24) can be asymptotically decomposed into the following two stages. The first one covers the fast process of heating and evaporation of the droplets. This stage is asymptotically characterized by the constant initial value of the gas temperature. The second stage refers to the classical fast ignition. As a result, the total time to final ignition can be estimated as:

$$\tau_{\text{ignition}} = \tau_{\text{droplets}} + \tau_{\text{induction}}, \tag{27}$$

where τ_{droplets} is the life time of the droplets, and $\tau_{\text{induction}}$ is the time required for the ignition described by Equation (26) to take place (induction time). The lifetime of the droplets τ_{droplets} is the time during which the phase trajectory reaches the invariant line $\theta_d = \theta_b$. This can be calculated by integrating Equation (23) from the initial value θ_{d0} up to the boiling value θ_b (assuming that the slow variable is fixed and equal to the initial value $\theta_g = 0$):

$$\tau_{\text{droplets}} = \frac{\left(\theta_b - \theta_{d0}\right)}{\varepsilon_3} \int\limits_{\theta_{d0}}^{\theta_b} \frac{r^2\left(\theta_d\right)}{\left(-\theta_d\right)\left(\theta_b - \theta_d\right)\left[1 + \varepsilon_4\left(\nu - 1\right) r^{b+1}\left(\theta_d\right)\right]} \mathrm{d}\theta_d. \tag{28}$$

The induction time $\tau_{\text{induction}}$ is the time during which the temperature reaches the critical pre-explosive values. It can be calculated using the classical approaches (see for example [41]). For systems without heat losses the induction time can be approximated by the adiabatic time (that is the time during which the temperature becomes infinite with no reactant consumption). This time for Equation (26) can be easily found:

$$\tau_{\text{induction}} \approx \tau_{\text{ad}} = \frac{\gamma}{\eta\left(0, \theta_b\right)} \int\limits_0^{\infty} \exp\left(-\theta_g\right) \mathrm{d}\theta_g = \frac{\gamma}{\eta\left(0, \theta_b\right)},$$

where $\eta\left(0, \theta_b\right)$ is given by Equation (19) with $\theta_g = 0$, $\theta_d = \theta_b$. Remembering the definition of $\eta\left(0, \theta_b\right)$ we can estimate the induction time as:

$$\tau_{\text{induction}} \approx \frac{\gamma \varepsilon_3}{\varepsilon_1} \left(\int\limits_{\theta_{d0}}^{\theta_b} r^3\left(s\right) \frac{\left(\psi_f\left(1 - \zeta\left(s\right)\right) - 1\right)}{\zeta\left(s\right)} \mathrm{d}s \right)^{-1}. \tag{29}$$

where $r^3(s)$ and $\zeta(s)$ are given by Equations (18) and (15) respectively.

4.2. THE CASE $\varepsilon_3\gamma/\varepsilon_1 \ll 1$

In this case initially θ_g is a rapidly varying variable, and θ_d is a slowly varying variable. The slow curve of the system of Equations (22)–(24) is defined by the quasi-steady-states of the fast Equation (22):

$$F\left(\theta_g, \theta_d\right) \stackrel{\text{def}}{=} H_{HR}^{FK}\left(\eta\left(\theta_g, \theta_d\right), \theta_g\right) - \varepsilon_1 r\left(\theta_d\right) \; H_{HL}^{\text{app}}\left(r\left(\theta_d\right), \theta_g, \theta_d\right) = 0. \tag{30}$$

Stability of the slow curve is controlled by the sign of $\left(\partial F \big/ \partial\theta_g\right)$. The turning point T($\theta_g = \theta_g^T$, $\theta_d = \theta_d^T$) at which

$$F = \partial F \big/ \partial\theta_g = 0 \tag{31}$$

separates the stable (attracting) part $\left(\partial F \big/ \partial\theta_g < 0\right)$ from the unstable (repelling) part $\left(\partial F \big/ \partial\theta_g > 0\right)$. Stability of the slow curve and the phase trajectory is illustrated in Figure 2. One can see that in the case under consideration, when cool droplets are injected into a hot gas $\left(\theta_{d0} < \theta_b < \theta_{g0} = 0\right)$, the phase trajectory can be divided into three parts IN, NT and TE. The initial part of the trajectory IN is a horizontal line connecting the initial point I$\left(\theta_g = 0, \theta_d = \theta_{d0}\right)$ with the point N$\left(\theta_g = \theta_{gi}, \theta_d = \theta_{d0}\right)$ on the stable part of the slow curve where θ_{gi} is given by

$$F\left(\theta_{gi}, \theta_{d0}\right) = 0\ . \tag{32}$$

The part IN describes the initial fast cooling of the gas from the initial zero θ_g down to the value θ_{gi} which is close to θ_{d0}. The system dynamics is then governed by the slow Equation (23) with $\theta_g = \theta_g\left(\theta_d\right)$ given by Equation (30). The corresponding part of the trajectory moves along the slow curve from the point N (defined by Equation (32)) until the turning point T (defined by Equation (31)). The last horizontal part of the trajectory TE describes the final ignition event. The rates of changes of the slow and the fast variables become comparable in the phase plane within a close neighborhood of the stable slow curve, due to a fine balance between the heat release and heat-loss mechanisms. Therefore, the trajectory part INT is responsible for the delay phenomena before the final ignition. The ignition time can be estimated using the trajectory parts IN and NT. The part IN describes the fast process of temperature cooling; therefore the impact of the corresponding time is negligible by comparison with the time of slow motion NT. As a result, the ignition time can be calculated from Equation (23) as:

$$\tau_{\text{ignition}} = \frac{\left(\theta_b - \theta_{d0}\right)}{\varepsilon_3} \int\limits_{\theta_{d0}}^{\theta_d^T} \frac{r^2\left(\theta_d\right)}{\left(\theta_g\left(\theta_d\right) - \theta_d\right)\left(\theta_b - \theta_d\right)\left[1 + \varepsilon_4\left(\nu - 1\right) r^{b+1}\left(\theta_d\right)\right]} \, \mathrm{d}\theta_d \tag{33}$$

with $\theta_g\left(\theta_d\right)$ given by slow curve of Equation (30) and θ_d^T given by Equation (31) (turning point T).

5. Discussion

Values of parameters in a diesel-engine combustion chamber vary widely. Our analysis will be focused on the zone located at a comparatively large distance from the injector (far zone) and

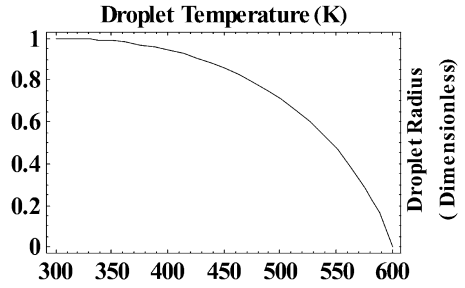

Figure 3. Dimensionless droplet radius $r = R_d/R_{d0}$ versus dimensional droplet temperature T_d as predicted by Equation (18).

the one close to it (near zone). The values of relative droplet volume fraction φ_d in the far zone are typically small ($\varphi_d < 0{\cdot}003$), while those in the near zone are much larger ($\varphi_d \gg 0{\cdot}003$). The value of $\varphi_d = 0{\cdot}003$ corresponds to the stoichiometric condition. The simple expression of the volumetric liquid-fuel content $\left(\varphi_d = \frac{4}{3}\pi\, n_d R_{d0}^3\right)$ allows us to choose the relevant values of the initial droplet radius R_{d0} and the droplet concentration n_d. The value $R_{d0} = 5\,\mu$m has been chosen for the far zone, while $R_{d0} = 50\,\mu$m has been chosen for the near zone. The values of n_d have been taken the same in both zones. The values of the other parameters are assumed the same for both zones [20, 13, 19]:

$$\begin{aligned}
&E = 7.6 \times 10^7\ (\mathrm{J\,kmol^{-1}}),\ \lambda_{g0} = 0{\cdot}061\ (\mathrm{W\,m^{-1}\,K^{-1}}),\ \rho_{g0} = 23{\cdot}8\,(\mathrm{kg\,m^{-3}}),\\
&C_{pg} = C_{pf_v} = 1120\ \left(\mathrm{J\,kg^{-1}K^{-1}}\right),\ T_{g0} = 900\,(\mathrm{K}),\ Q_f = 4{\cdot}3 \times 10^7\ (\mathrm{Jkg^{-1}}),\\
&\sigma = 5{\cdot}67 \times 10^{-8}\,(\mathrm{W\,m^{-2}\,K^{-4}}),\ b = 0{\cdot}6,\ \kappa_{01} = 0{\cdot}28,\ \kappa_{11} = 0{\cdot}08,\ T_b = 600\,(\mathrm{K}),\\
&T_{d0} = 300\,(\mathrm{K}),\ C_d = 2830\ \left(\mathrm{J\,kg^{-1}K^{-1}}\right),\ L = 3{\cdot}6 \times 10^5\ (\mathrm{J\,kg^{-1}}),\\
&\rho_{d0} = 600\,(\mathrm{kg\,m^{-3}}),\ \mu_f = 170\,(\mathrm{kg\,kmol^{-1}}),\ A = 3 \times 10^6\,(\mathrm{s^{-1}}),\ n_d = 8 \times 10^{11}\ (\mathrm{m^{-3}})
\end{aligned} \tag{34}$$

The corresponding dimensionless parameters for the two zones are given below.

'Far zone':

$$\begin{aligned}
&\varphi_d = 4{\cdot}18879 \times 10^{-4},\quad \varepsilon_1 = 2{\cdot}16986 \times 10^{-1},\quad \varepsilon_2 = 1{\cdot}19394 \times 10^2,\\
&\varepsilon_3 = 3{\cdot}721 \times 10^1,\ \varepsilon_4 = 6{\cdot}43762 \times 10^{-4},\ \gamma = 2{\cdot}18454 \times 10^{-1}
\end{aligned} \tag{35}$$

'Near zone':

$$\begin{aligned}
&\varphi_d = 4{\cdot}18879 \times 10^{-1},\ \varepsilon_1 = 3{\cdot}73236 \times 10^{-3},\ \varepsilon_2 = 6{\cdot}94117 \times 10^1,\\
&\varepsilon_3 = 3{\cdot}721 \times 10^{-1},\ \varepsilon_4 = 2{\cdot}56286 \times 10^{-2},\ \gamma = 2{\cdot}18454 \times 10^{-4}
\end{aligned} \tag{36}$$

The following dimensionless parameters are the same for both zones:

$$\beta = 9{\cdot}84079 \times 10^{-2},\ \psi_f = 1{\cdot}19444 \times 10^2,\ \varepsilon_5 = 2{\cdot}8,\ \nu = 3{\cdot}88889. \tag{37}$$

The plot of the dimensionless droplet radius (r) *vs.* the dimensional droplet temperature (T_d), based on Equation (18) is presented in Figure 3 (it refers to both zones). The power $\varepsilon_1\varepsilon_2/\varepsilon_3$ in Equation (18) represents the ratio$T_{g0}\beta\, C_d/L$.

The analysis was conducted for $\varepsilon_3\gamma/\varepsilon_1 \gg 1$ and $\varepsilon_3\gamma/\varepsilon_1 \ll 1$. These conditions are typical for the far and near zones, respectively.

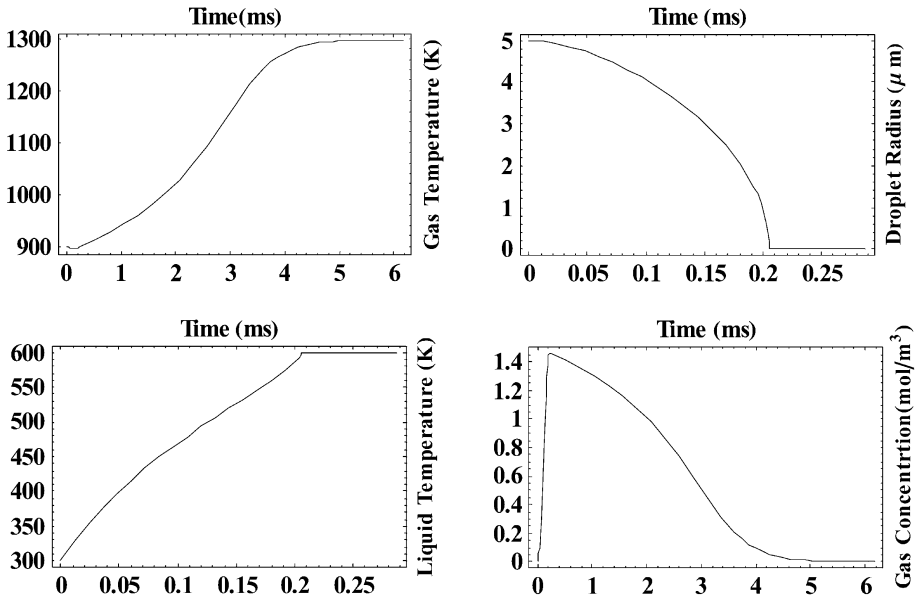

Figure 4. Time histories of variables for the far zone (the values of parameters are specified in Section 4).

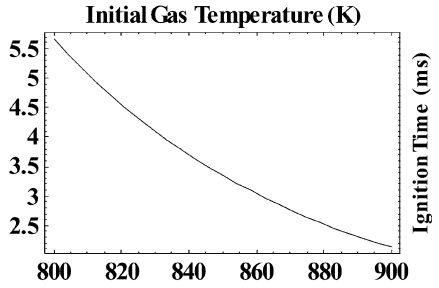

Figure 5. Ignition time delay versus the initial gas temperature for the far zone, as predicted by Equations (27)–(29).

5.1. FAR ZONE (SMALL DROPLET CONCENTRATION)

The plots of time histories of gas temperature, liquid-fuel temperature, droplet radius and fuel-vapor concentration obtained from the numerical solution of Equations (9)–(12), (17) with the dimensionless parameters (35), (37) are presented in Figure 4. The sharp increase in gas temperature and fuel-vapor concentration at times close to 2 ms indicates the explosive behavior of the system. On the other hand, droplet evaporation time (about 0·2 ms) is small and can be effectively ignored when estimating the overall ignition-delay time. The results of numerical simulations are in agreement with Equations (27)–(29), which predict a total ignition-delay time of about 2·1 ms. Also, the droplet-evaporation time inferred from Figure 4 agrees with the prediction of Equation (28). The latter gives a value of about 0·2 ms. The induction time predicted by Equation (29) is about 1·9 ms. This may justify the application of Equations (27)–(29) to the analysis of the dependences of the ignition time on the key system parameters. The plot of ignition time *vs.* initial gas temperatures as predicted by the theoretical results (27)–(29) is shown in Figure 5. The decrease of ignition time with increase of initial

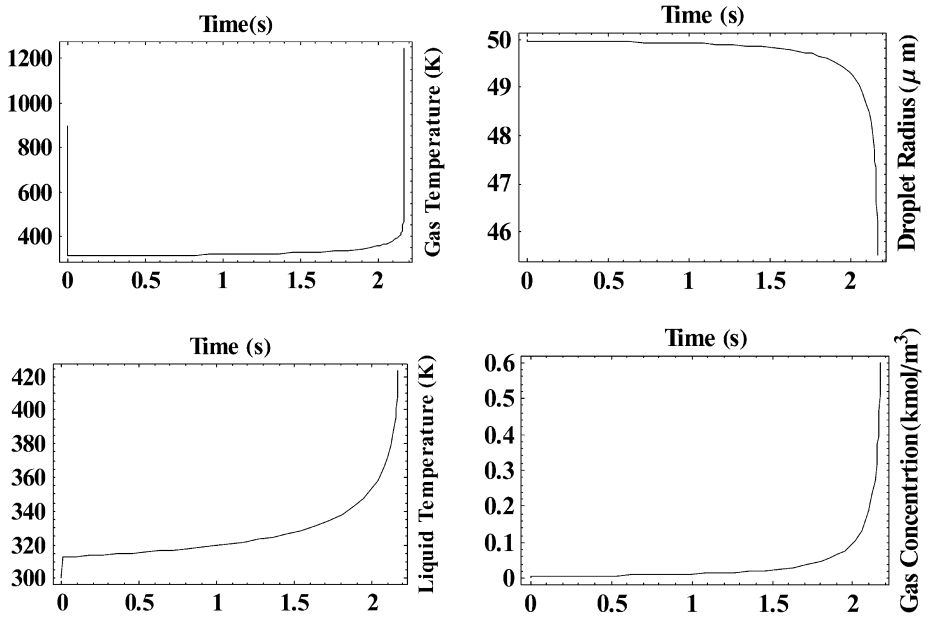

Figure 6. Time histories of variables for the near zone (the values of parameters are specified in Section 4).

gas temperature predicted by this figure is consistent with predictions of CFD calculations [13].

Rather small values of τ_{droplets} predicted by the analysis are related to the assumption about a well-stirred mixture of fuel vapor and air in the vicinity of the droplets. If the gradient of the gas temperature in the vicinity of the droplets is taken into account, the temperature of gas in the immediate vicinity of droplets would drop to about 670 K. The droplet-evaporation time for this temperature, as predicted by Equation (28) would be about 0.8 ms. This agrees with the results of CFD calculations [19]. The values of τ_{ignition} shown in Figure 5 are slightly higher than the ones predicted by a CFD analysis (1–3 ms). This can be related to the assumption of the Arrhenius-type chemical term in the energy equation [13]. Our simplified model, however, correctly predicts two important features of the phenomenon. These are the small relative contribution of τ_{droplets} in τ_{ignition} for small droplets and decrease of τ_{ignition} with increasing T_{g0}.

5.2. NEAR ZONE (HIGH DROPLET CONCENTRATION)

The plots of time histories of gas temperature, liquid-fuel temperature, droplet radius and fuel-vapor concentration, obtained from the numerical solution of Equations (9)–(12), (17) with the values of dimensionless parameters given by Equations (36) and (37), are shown in Figure 6. As can be seen from this figure, the time of thermal explosion of gas almost coincides with the time of droplet heating and evaporation. The ignition time delay in the near zone (about 2·2 s) indicates that ignition actually does not take place here. Large droplets are likely to break up and be removed from the near zone during this time. Also, the ignition in the far zone is likely to modify the condition for the explosion in the near zone (the initial gas temperature is likely to increase above 2500 K). Analysis of these events is beyond the scope of this paper.

5.3. Effect of radiation on the ignition time

The relative effect of thermal radiation on the total heat transfer to droplets is controlled by the term $\varepsilon_4 (\nu - 1)\ r^{b+1}$ in the heat-loss term H_{HL} given by Equation (21). Assuming that $r = 0{\cdot}5$ to account for droplet evaporation, and remembering Equations (35)–(37) we obtain $\varepsilon_4 (\nu - 1)\ r^{b+1} = 0{\cdot}0006$ for the far zone and $\varepsilon_4 (\nu - 1)\ r^{b+1} = 0{\cdot}024$ for the near zone. This means that the relative effect of thermal radiation is negligible for small droplets in the far zone, but may be important for large droplets in the near zone. This effect would increase at the initial stage of evaporation when r is close to one and for larger droplets. Note that the total ignition delay in the far zone is relatively insensitive to the values of combined convection and radiation heat coefficients. As follows from Equations (27)–(29), the increase of the combined heat-transfer coefficient by 0·06% due to the contribution of thermal radiation would decrease the total ignition delay time by less than 0·01%. The decrease of the ignition delay time in the near zone as estimated from Equation (33) would be about 2·4% as estimated above. This conclusion, however, is essentially based on the assumption that the gas is optically thick and the temperature responsible for radiation (radiation temperature) is equal to the gas temperature. In the general case, in a diesel-engine environment, the former temperature can be substantially larger than the latter. In this case the effect of thermal radiation would be expected to be the dominant (see [42] for details).

6. Conclusions

The problem of thermal explosion in a flammable gas mixture with the addition of volatile fuel droplets has been studied based on the asymptotic method of integral manifolds. Both convective and radiative heating of droplets is accounted for. The model for radiative heating has taken into account the semitransparency of droplets. A simplified model for droplet heat-up has been used. The mathematical model has been presented as a singularly perturbed system of four highly nonlinear ordinary differential equations involving energy and concentration relations for the gas phase, energy equation for the liquid phase and droplets mass-balance relation. The results of the analysis have been applied to the modelling of thermal explosion in diesel engines. Two distinct dynamic situations have been considered depending on the initial droplet concentration. These are ‘far zone’ (small initial liquid-volume fraction and small droplet radii) and ‘near zone’ (large initial liquid-volume fraction and large droplet radii). The conditions of the first zone are typical for areas in the combustion chamber that are far from the spray injectors, while the conditions of the second zone are typical for those areas in the combustion chamber that are relatively close to the spray injectors. In agreement with predictions of CFD calculations, it has been pointed out that the time of small (radii less or equal to 5 μm) droplets heating and evaporation in the far zone is smaller than the chemical ignition delay of the fuel-vapor/air mixture. Also, in agreement with CFD predictions, the total ignition delay is shown to decrease with increase of the initial gas temperature. In the near zone for large (radii greater or equal to 50 μm) droplets the process has been shown to start with a fast initial gas cooling and slight heating of droplets. This is followed by a relatively slow heating of the gas due to chemical reaction and further droplet heating. The total ignition delay in the near zone has been shown to be larger than in the far zone. It is expected that, before thermal explosion in the near zone takes place, the droplets break up and are removed from this zone. Also, the whole process is likely to be affected by the explosion

in the far zone. In optically thick gas effects of thermal radiation are shown to be negligible for small droplets but are noticeable for large droplets.

Acknowledgements

The authors would like to thank Vladimir Sobolev for important comments on the draft version of the paper, and Olga Dolgova for the derivation of Equation (18). Ann Zinoviev and Igor Goldfarb are grateful to the Guastella Foundation and the German-Israeli Foundation (Grant G-695-15.10/2001), respectively, for financial support. Sergei Sazhin is grateful to the Israeli Ministry of Science and the British Council for financial support of his visit to Israel in December 2001 when the work on this paper was started.

References

1. K.K. Kuo, *Principles of Combustion.* New York: John Wiley & Sons (1986) 810 pp.
2. S.K. Aggarwal, A review of spray ignition phenomena: present status and future research. *Prog. Energy Combust. Sci.* 24 (1998) 565–600.
3. N.N. Semenov, Zur Theorie des Verbrennungsprozesses. *Z. Phys. Chem.* 48 (1928) 571–581.
4. W.A. Sirignano, R.H. Rangel, D. Dunn-Rankin, M.E. Orme, Generation, vaporization, and combustion of droplet arrays and streams. In: K.K. Kuo (ed.), *Recent Advances in Spray Combustion: Spray Atomization and Drop Burning Phenomena, Volume 1* Amer. Inst. Aeron. Astron. (1996) pp. 327–380.
5. G.L. Borman and K.W. Ragland, *Combustion Engineering.* New York: WCB and McGraw-Hill (1998) 613 pp.
6. H. Pitsch and N. Peters, Investigation of the ignition process of sprays under Diesel engine conditions using reduced n-heptane chemistry. *SAE Technical Paper SAE2464*, Society of Automotive Engineers, U.S.A. (1998).
7. W.A. Sirignano, *Fluid Dynamics and Transport of Droplets and Sprays* Cambridge: CUP (1999) 308 pp.
8. H.H. Chiu and L.H. Hu, Dynamics of ignition transience and gasification partition of a droplet. *Proc. Combust. Inst.* 27 (1999) 1889–1996.
9. P. Stapf, H.A. Dwyer and R.R. Maly, A group combustion model for treating reactive sprays in I.C. engines. *Proc. Combust. Inst.* 27 (1999) 1857–1864.
10. H. Barth, C. Hasse and N. Peters, Computational fluid dynamics modelling of non-premixed combustion in direct injection diesel engines. *Int. J. Engine Res.* (2000) 249–267.
11. R.D. Reitz and C.J. Rutland, Development and testing of Diesel engine CFD models. *Prog. Energy Combust. Sci.* 21 (1995) 173–196.
12. S-C. Kong, Z. Han and R.D. Reitz, The development and application of a Diesel ignition and combustion model for multidimensional engine simulation. *SAE Technical Paper SAE950278*, Society of Automotive Engineers, U.S.A. (1996).
13. E.M. Sazhina, S.S. Sazhin, M.R. Heikal, V.I. Babushok and R. Johns, A detailed modelling of the spray ignition process in Diesel engines. *Combust. Sci. Technol.* 160 (2000) 317–344.
14. V. Gol'dshtein and V. Sobolev, Integral manifolds in chemical kinetics and combustion. In: *Singularity Theory and Some Problems of Functional Analysis.* AMS Translations, Series 2, 153 (1992) pp. 73–92.
15. A.C. McIntosh, V. Gol'dshtein, I. Goldfarb and A. Zinoviev, Thermal explosion in a combustible gas containing fuel droplets. *Combust. Theory Modell.* 2 (1998) 153–165.
16. I. Goldfarb, V. Gol'dshtein, G. Kuzmenko and S.S. Sazhin, Thermal radiation effect on thermal explosion in gas containing fuel droplets. *Combust. Theory Modell.* 3 (1999) 769–787.
17. I. Goldfarb, V. Gol'dshtein, B.J. Grenberg and G. Kuzmenko, Thermal radiation effect on thermal explosion in gas containing fuel droplets. *Combust. Theory Modell.* 4 (2000) 289–316.
18. V. Bykov, I. Goldfarb, V. Gol'dshtein and J.B. Greenberg, Thermal explosion in a hot gas mixture with fuel droplets: a two reactants model. *Combust. Theory Modell.* 2 (2002) 153–165.
19. S.S. Sazhin, G. Feng, M.R. Heikal, I. Goldfarb, V. Gol'dshtein and G. Kuzmenko, Thermal ignition analysis of a monodisperse spray with radiation. *Combust. Flame* 124 (2001) 684–701.

20. P.F. Flynn, R.P. Durrett, G.L. Hunter, A.O. zur Loye, O.C. Akinyemi, J.E. Dec and C.K. Westbrook, Diesel combustion: an integrated view combining laser diagnostics, chemical kinetics, and empirical validation. *SAE Technical Paper SAE report 1999-01-0509*, Society of Automotive Engineers, U.S.A. (1999).
21. V.Ya. Basevich, Chemical kinetics in the combustion processes. In: N.P. Cheremisinoff (ed.), *Handbook of Heat and Mass Transfer. Advances in Reactor Design and Combustion Science.* Houston: Gulf Publishing Company (1990) 769–819.
22. K. Sahetchian, J.C. Champoussin, M. Brun, N. Levy, N. Blin-Simiand, C. Aligrot, F. Jorand, M. Socoliuc, A. Heiss and N. Guerassi, Experimental study and modeling of dodecane ignition in a Diesel engine. *Combust. Flame* 103 (1995) 207–220.
23. R. Minetti, M. Ribaucour, M. Carlier and L.R. Sochet, Autoignition delays of a series of linear and branched chain alkanes in the intrmediate range of temperature. *Combust. Flame* 113–114 (1996) 179–192.
24. R. Minetti, A. Roubaud, E. Therssen, M. Ribaucour and L.R. Sochet, The chemistry of pre-ignition of n-pentane and 1-pentene. *Combust. Flame* 118 (1999) 213–220.
25. U.C. Müller, N. Peters and A. Liñan, Global kinetics for n-heptane ignition at high pressures. In: *Proceedings of the Combustion Institute* 24 (1992) 777–784.
26. V.Ya. Basevich and S.M. Frolov, A reduced kinetic scheme for autoignition modelling of iso-octane and n-heptane air mixtures during the induction period for internal combustion engines. *Chem. Phys.* 13 (1994) 146–156 (in Russian).
27. J.F. Griffiths, Reduced kinetic models and their application to practical combustion systems. *Prog. Energy Combust. Sci.* 21 (1995) 25–107.
28. M. Halstead, L. Kirsh and C.P. Quinn, The autoignition of hydrocarbon fuels at high temperatures and pressures – fitting of a mathematical model. *Combust. Flame* 30 (1977) 45–60.
29. P.L.C. Lage and R.H. Rangel, Single droplet vaporization including thermal radiation and absorption. *J. Thermophys. and Heat Transfer* 7 (1993) 502–509.
30. L.A. Dombrovsky, *Radiation Heat Transfer in Disperse Systems.* New York, Wallingford: Begell House Inc (1996) 256 pp.
31. L.A. Dombrovsky, S.S. Sazhin, E.M. Sazhina, G. Feng, M.R. Heikal, M.E.A. Bardsley and S.V. Mikhalovsky, Heating and evaporation of semi-transparent Diesel fuel droplets in the presence of thermal radiation. *Fuel* 80 (2001) 1535–1544.
32. S.S. Sazhin, P.A. Krutitskii, W.A. Abdelghaffar, E.M. Sazhina, S.V. Mikhalovsky, S.T. Meikle and M.R. Heikal, Transient heating of diesel fuel droplets. *Int. J. Heat Mass Transfer* (2004) in press.
33. I. Goldfarb, V. Gol'dshtein and A. Zinoviev, Delayed thermal explosion in porous media: method of invariant manifolds. *IMA J. Appl. Math.* 67 (2002) 263–280.
34. S.S. Sazhin, G. Feng and M.R. Heikal, A model for fuel spray penetration. *Fuel* 80 (2001) 2171–2180.
35. R.B. Bird, W.E. Stewart and E.N. Lightfoot, *Transport Phenomens.* New York: John Wiley & Sons (2002) 895 pp.
36. Z-G. Feng and E.E. Michaelides, Heat and mass transfer coefficient of viscous spheres. *Int. J. Heat Mass Transfer* 44 (2001) 4445–4454.
37. S.H. Sohrab, A. Linan and F.A. Williams, Asymptotic theory of diffusion-flame extinction with radiant loss from the flame zone. *Combust. Sci. Technol.* 27 (1982) 143–154.
38. I. Goldfarb, V. Gol'dshtein, B.J. Greenberg and G. Kuzmenko, Analysis of radiative heat-loss effects in thermal explosion of a gas using the integral manifold metod. *J. Engng. Math.* 44 (2002) 229–243.
39. S.S. Sazhin, W.A. Abdelghaffar, E.M. Sazhina, S.V. Mikhalovsky, S.T. Meikle and C. Bai, Radiative heating of semi-transparent diesel fuel droplets. *ASME J. Heat Transfer* (2004) in press.
40. S.S. Sazhin, L.A. Dombrovsky, P. Krutitskii, E.M. Sazhina and M.R. Heikal, Analytical and numerical modelling of convective and radiative heating of fuel droplets in diesel engines. In: J. Taine (ed.), *Proc. Twelfth Int. Heat Transfer Conf.* (2002) pp. 699–704.
41. D.A. Frank-Kamenetskii, *Diffusion and Heat Exchange in Chemical Kinetics*. New-York: Plenum Press (1969) 574 pp.
42. E.M. Sazhina, S.S. Sazhin, M.R. Heikal and M.E.A. Bardsley, The P-1 model for thermal radiation transfer: application to numerical modelling of combustion processes in Diesel engines. In: R. Vichnevetsky *et al.* (ed.), *Proceedings of the 16th IMACS World Congress 2000 on Scientific Computation, Applied Mathematics and Simulation* CD (paper 125-10), 2000.